Cell, Vol. 95, 163–175, October 16, 1998, Copyright ©1998 by Cell Press

# Nef Harbors a Major Determinant of Pathogenicity for an AIDS-like Disease Induced by HIV-1 in Transgenic Mice

**Zaher Hanna,[1,2,7,8] Denis G. Kay,[1,8] Najet Rebai,[1] Alain Guimond,[1] Serge Jothy,[4,6] and Paul Jolicoeur[1,3,5,7]**
[1]Laboratory of Molecular Biology
Clinical Research Institute of Montreal
Montreal, Quebec, H2W 1R7
Canada
[2]Department of Medicine
[3]Department of Microbiology and Immunology
Université de Montréal
Montreal, Quebec, H3C 3J7
Canada
[4]Department of Pathology
[5]Department of Experimental Medicine
McGill University
Montreal, Quebec, H3G 1A4
Canada
[6]Department of Laboratory Medicine
and Pathology
University of Toronto
Toronto, Ontario, M5G 1L5
Canada

## Summary

**Transgenic (Tg) mice expressing the complete coding sequences of HIV-1 in CD4$^+$ T cells and in cells of the macrophage/dendritic lineages develop severe AIDS-like pathologies: failure to thrive/weight loss, diarrhea, wasting, premature death, thymus atrophy, loss of CD4$^+$ T cells, interstitial pneumonitis, and tubulo-interstitial nephritis. The generation of Tg mice expressing selected HIV-1 gene(s) revealed that nef harbors a major disease determinant. The latency and progression (fast/slow) of the disease were strongly correlated with the levels of Tg expression. Nef-expressing Tg thymocytes were activated and $\alpha$-CD3 hyperresponsive with respect to tyrosine phosphorylation of several substrates, including LAT and MAPK. The similarity of this mouse model to human AIDS, particularly pediatric AIDS, suggests that Nef may play a critical role in human AIDS, independently of its role in virus replication.**

## Introduction

Infection of humans with HIV-1 induces a severe disease designated AIDS (for review see Pantaleo and Fauci, 1995). AIDS is characterized by a gradual depletion of CD4$^+$ T cells, and the disease is often associated with other pathologies thought to be caused by HIV-1 infection rather than by opportunistic infections. These include interstitial lymphocytic pneumonitis (predominately observed in children) (McSherry, 1996), tubulo-interstitial nephritis, and/or glomeruloslerosis (Seney et al., 1990), wasting (Coodley et al., 1994), heart disease (Herskowitz, 1996), and central (CNS) and peripheral nervous system diseases (Price, 1996).

High viral load has been associated with faster progression to and a more severe form of AIDS (Ho, 1996). In the context of virus replication, it has been difficult to determine the effect of each of the viral gene products on cellular functions and their contribution to the development of AIDS. This has been best studied in animal models, in Tg mice expressing subsets of HIV-1 genes in specific tissues. These Tg mice were reported to exhibit pathological lesions resembling some of those found in individuals with AIDS, such as nephropathy, CNS changes, thymic atrophy, and CD4$^+$ T cell depletion, while others (such as cataracts and epidermal hyperplasia) are not usually observed in human AIDS (for review see Klotman et al., 1995). However, none of these Tg mice developed an immune syndrome that closely resembled human AIDS, perhaps reflecting the lack of Tg expression in relevant target cells.

To address this problem, we have previously constructed Tg mice expressing the whole coding sequences of HIV-1 under the regulatory sequences of the human CD4 (CD4C) gene, in the same subsets of cells as those normally found to be infected in HIV-1-infected individuals, namely immature CD4$^+$CD8$^+$ thymic T cells, mature CD4$^+$CD8$^-$ T cells, and cells of the monocyte/macrophage lineage (Hanna et al., 1998). These CD4C/HIV$^{wt}$ Tg mice developed a very severe AIDS-like disease with several features remarkably similar to those reported in humans infected with HIV-1 (Hanna et al., 1998). These included severe immune disease (with thymic atrophy, loss of peripheral T-lymphocytes, and loss of architecture of lymphoid organs), failure to thrive and/or weight loss, wasting, diarrhea, interstitial lymphocytic pneumonitis, tubulo-interstitial nephritis, and premature death.

To determine the contribution of individual HIV-1 genes in the pathogenesis of this AIDS-like disease of CD4C/HIV$^{wt}$ Tg mice, we mutated selected HIV-1 genes and constructed five mutant CD4C/HIV DNAs, which were assayed in 18 lines of Tg mice. These studies revealed that *nef* harbors a major determinant of pathogenicity.

## Results

### Generation of Tg Mice Harboring Mutant HIV-1 Genes

Five HIV-1 mutant DNAs (CD4C/HIV$^{MutA}$, CD4C/HIV$^{MutB}$, CD4C/HIV$^{MutC}$, CD4C/HIV$^{MutG}$, and CD4C/HIV$^{MutH}$) were constructed for the present study (Figure 1A). The same regulatory elements of the human CD4 gene (CD4C) used in our previous studies (Hanna et al., 1994, 1998) were used to drive the expression of these different genes. All these transgenes were constructed on the

[7]To whom correspondence should be addressed (e-mail: jolicop@ircm.umontreal.ca [P. J.]).
[8]These authors contributed equally to this work.

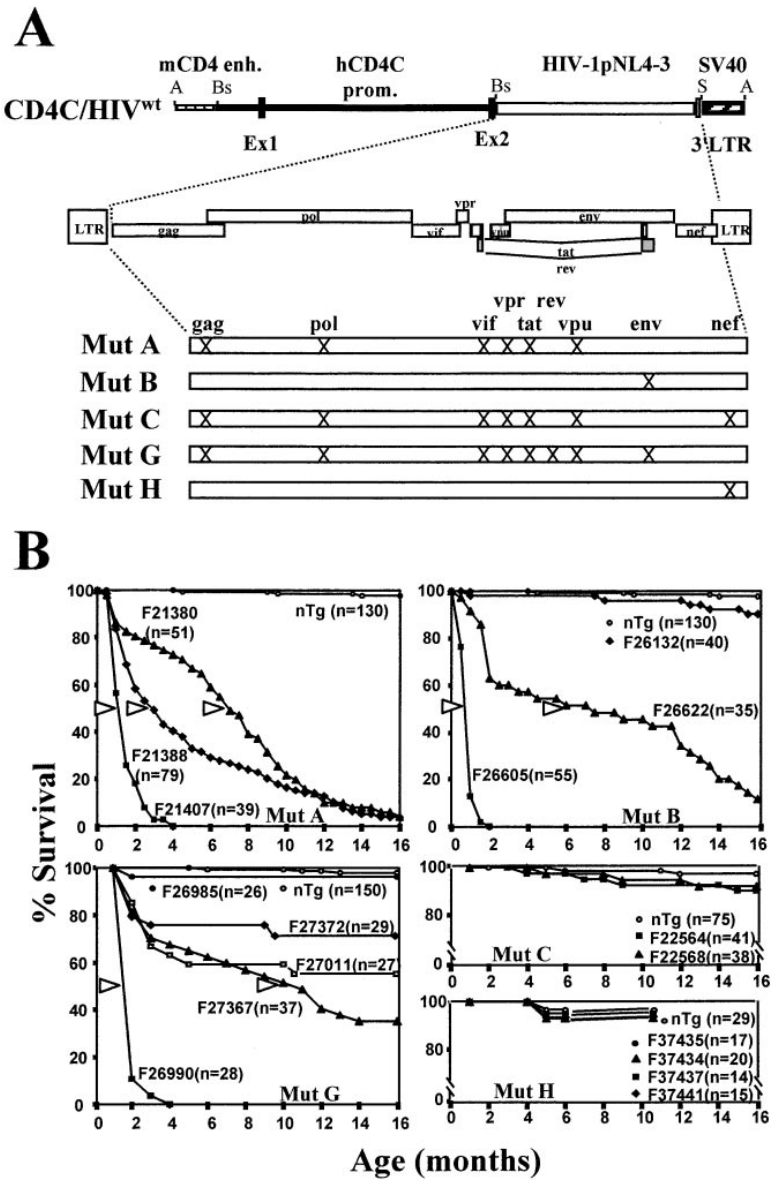


Figure 1. Incidence of Death in CD4C/HIV$^{Mut}$ Tg Mice

(A) Structure of the CD4C/HIV$^{Mut}$ transgenes. The mouse CD4 enhancer (mCD4enh), the human CD4 promoter (hCD4C prom.), each of the HIV-1$^{NL4-3}$ mutant genomes, and the polyadenylation sequences from simian virus 40 (SV40) were ligated. Ex1 and 2 are the first two untranslated exons of the hCD4 gene; 3′LTR is part of the 3′LTR of the HIV-1 genome. The symbol (X) means that the ORF of the indicated HIV gene was interrupted. Restriction sites: A, AatII; Bs, BssHII; S, SstI.
(B) Cumulative incidence of death in non-Tg and CD4C/HIV$^{Mut}$ Tg mice. The arrows show the time of death of 50% ($TD_{50}$) of the Tg mice for each mutant. Each point represents the death of a mouse. Symbols: n = number of animals observed.

same DNA backbone to make comparisons between them more valid. At least two to four Tg mouse lines were established with each of these DNA constructs. All founder (F) mice were bred on the C3H background, and progeny mice were genotyped and routinely examined for signs of disease.

### Clinical Phenotypes of CD4C/HIV$^{Mut}$ Mice

A fatal disease very similar to the one described in the CD4C/HIV$^{wt}$ Tg mice (Hanna et al., 1998) developed in mice originating from two or more founders harboring the CD4C/HIV$^{MutA}$, CD4C/HIV$^{MutB}$, or CD4C/HIV$^{MutG}$ DNA. The diseases induced by these three DNAs appeared similar and exhibited a distinct latency and penetrance according to the levels of Tg expression (see below). A high proportion (~38%) of high-expresser mice had diarrhea and edema, and most (>90%) developed weakness, hypoactivity, and wasting. Wasting was the most prevalent phenotype observed in these high-expresser mice. At 3 weeks of age, the body weight of non-Tg and Tg mice from different founders (MutA, F21407; MutB, F26605) was indistinguishable (non-Tg: 11.2 ± 3 g [n = 5]; Tg: 10.5 ± 2.2 g [n = 11]). However, by the end of the fourth week, in more severely affected mice, the body weight of Tg mice (8.7 ± 1.7 g [n = 11]) was much lower than that of non-Tg littermates (17.9 ± 3.3 g [n = 5]). In mice expressing moderate levels of the Tg, these phenotypes appeared less frequently and later in life. None of the control non-Tg littermates (n = 514) kept in the same cages as the Tg mice, nor those mice harboring the CD4C/HIV$^{MutC}$, nor CD4C/HIV$^{MutH}$ Tg (n = 145) developed a similar disease.

### CD4C/HIV$^{MutA}$ Tg Mice

Three CD4C/HIV$^{MutA}$ founders (F21380, F21388, and F21407) transmitted the Tg to their N1 progeny. Most N1 progeny from founder F21407 became sick and died early, within the first 45 days of life (Figure 1B). A few N2 mice were

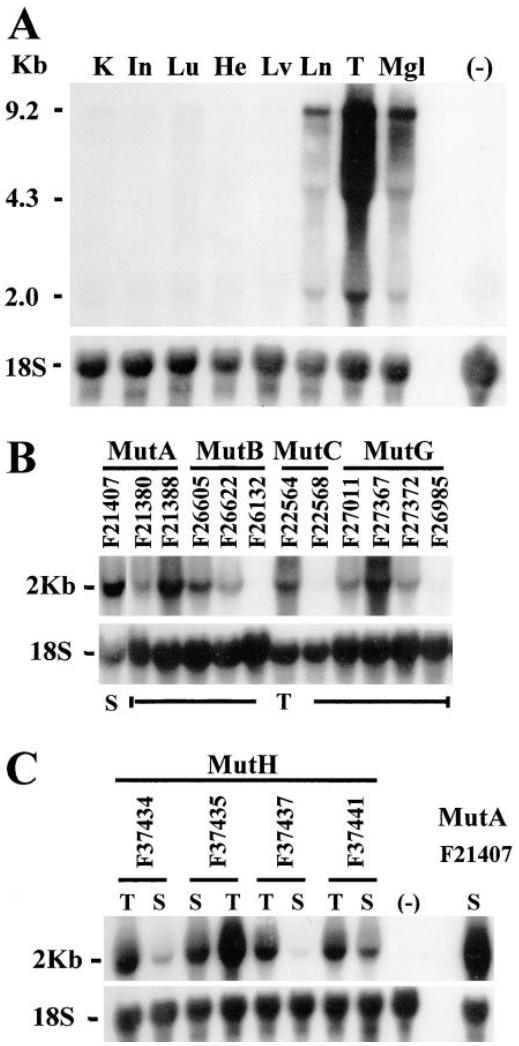


Figure 2. Expression of HIV-1 RNA in CD4C/HIV$^{Mut}$ Tg Mice

Northern blot analysis of HIV-1 RNA in various tissues of CD4C/HIV$^{Mut}$ Tg mice.

(A) Total RNAs (10 μg) extracted from different organs of CD4C/HIV$^{MutA}$ (F21407) mice were hybridized with a $^{32}$P-labeled HIV-1-specific 3′ end probe.

(B and C) Comparison of the levels of RNA expression of mice from different founder Tg lines was based on the intensity of the 2 kb transcript hybridizing with a $^{32}$P-labeled HIV-1 nef-specific probe. The filters were then washed and rehybridized with the 18S ribosomal specific probe.

Symbols: He, heart; In, Intestine; K, Kidney; Ln, lymph node; Lv, liver; Lu, lung; S, Spleen; T, thymus; Mgl, mammary glands of a MMTV/HIV Tg mouse used as a positive control; (−), Thymus from a normal mouse.

born, but these also became moribund early in life, and a line could not be established. However, Tg lines could be established from founders F21380 and F21388 mice. The life span of the Tg animals from these lines was more variable, and the disease developed between 30 days and 16 months (Figure 1B). The latency of the disease reflected the levels of Tg expression (see below, Figures 2 and 3), being shorter in mice from founder F21407 than in mice from founders F21380 or F21388. These results indicated that several HIV-1 genes (*gag*, *pol*, *vif*, *vpr*, *tat*, and *vpu*) were dispensable to elicit this severe AIDS-like disease and that either *rev*, *env*, or *nef* (or a combination of them) was causing this profound phenotype.

### CD4C/HIV$^{MutB}$ Tg Mice

To determine if *env* made an important contribution to this disease, three CD4/HIV$^{MutB}$ founder mice (F26132, F26605, and F26622), harboring an HIV-1 genome with only the *env* gene inactivated, were produced. Tg offspring from two of these founders (F26605 and F26622) developed a disease similar to that observed in CD4C/HIV$^{MutA}$ mice, including early death. Again the penetrance of disease varied and correlated well with the levels of Tg expression (see below, Figures 2 and 3). All of the Tg progeny from the high-expresser founder F26605 died early (<2 months) (Figure 1B), while Tg mice from the medium-expresser F26622 line died at a later time (Figure 1B). Interestingly, animals of the F26132 line did not develop disease (Figure 1B), most likely as a result of the very low levels of expression of the Tg (see below). The capacity of the CD4C/HIV$^{MutB}$ DNA to elicit disease indicated that the HIV-1 *env* gene was dispensable for the appearance of this phenotype.

### CD4C/HIV$^{MutC}$ Tg Mice

The CD4C/HIV$^{MutC}$ DNA harbored only two intact HIV-1 genes (*rev* and *env*). Two founders (F22564 and F22568) were produced with this construct. No detectable phenotype was apparent in these founder mice or in their offspring (n = 81) during a period of observation of 23 months, although high levels of Tg expression were detected in one of them (see below). The inability of this Tg to induce a similar phenotype to that seen in CD4C/HIV$^{MutA}$ and CD4C/HIV$^{MutB}$ mice suggested that the *nef* gene, and not the *rev* or *env* gene, harbors the determinant of pathogenicity.

### CD4C/HIV$^{MutG}$ Tg Mice

To extend these data and confirm that indeed the *nef* gene was implicated in this disease, Tg mice harboring only the *nef* gene intact were constructed. Six founders were obtained, and Tg lines could be established with four founders (F26985, F27011, F27367, and F27372) but not from founders F26990 and F27357, whose offspring died at an early age. Offspring from all founders, except from F26985, developed a disease similar to that observed in CD4C/HIV$^{MutA}$ or CD4C/HIV$^{MutB}$ mice. The latency of disease varied among different lines (in the order F26990 >> F27367 >> F27011> F27372 > F26985) according to the levels of HIV-1 expression (see below, Figures 2 and 3). This latency was very short (30–50 days) in mice from founders F26990 (Figure 1B) and F27357 (data not shown) expressing the Tg at highest levels (see below). The absence of an obvious phenotype in mice from founder F26985 is likely to reflect the low level of Tg expression in this line (see below). The development of this severe disease in CD4C/HIV$^{MutG}$ mice, harboring a single known HIV-1 gene intact, the *nef* gene, indicated that *nef* harbors a major determinant responsible for this phenotype.

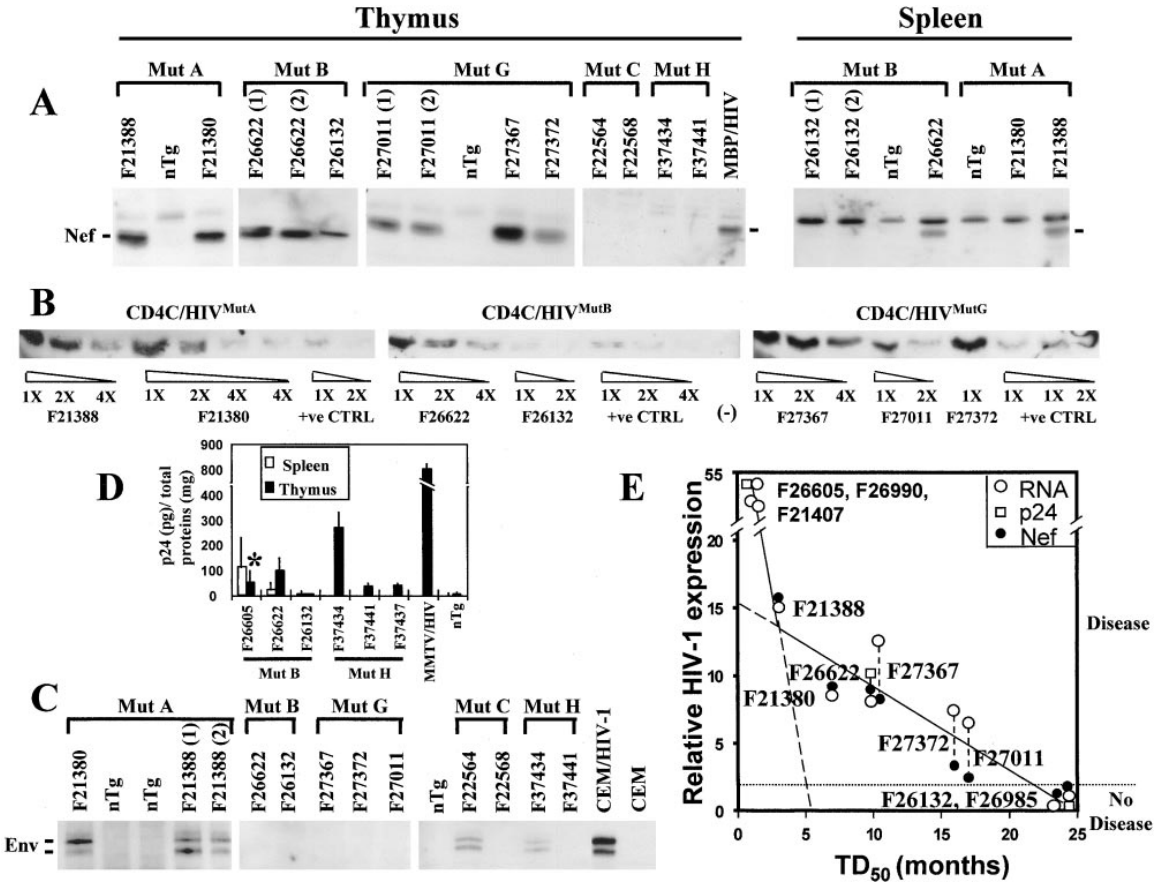


Figure 3. Expression HIV-1 Proteins in CD4C/HIV$^{Mut}$ Tg Mice

Total protein extracts (75 μg) from thymuses and spleens of one-month-old Tg and non-Tg littermates were separated by SDS-PAGE and analyzed by Western blotting with antibodies specific for HIV-1 Nef (A and B) or Env (C). CEM cells infected with HIV-1$^{LAV}$ and brain from MBP/HIV Tg mice (Goudreau et al., 1996) were used as positive controls. (B) Semiquantitative analysis of Nef proteins. Thymic extracts were serially diluted and compared to brain extracts from MBP/HIV Tg mice used as a standard for quantitation. (D) HIV-1 p24 proteins in CD4C/HIV$^{Mut}$ Tg mice. (*) These thymuses were already atrophied and partially exhausted. (E) Correlation between the time of death ($TD_{50}$) of CD4C/HIV$^{MutA}$, CD4C/HIV$^{MutB}$, and CD4C/HIV$^{MutG}$ Tg mice, as determined in Figure 1B for 11 independent Tg lines and levels of HIV-1 expression. The relative amounts of Nef, p24 (see B and D above), and RNA (Figure 2) obtained by densitometer scanning were used to draw these curves.

### CD4C/HIV$^{MutH}$ Tg Mice

To confirm that all the HIV-1 genes other than *nef* had a limited contribution in the development of these phenotypes, we produced the CD4C/HIV$^{MutH}$ Tg mice, with the complete HIV-1 coding sequences intact and only the *nef* gene mutated. Four founders were obtained (F37434, F37435, F37437, and F37441), and Tg lines were established. Although the levels of Tg expression in some of these lines were as high as those found in other lines developing disease (Figure 2), no obvious phenotype could be detected in these Tg mice (n = 70) during a 10−month latency period. This result confirmed our previous observations that *nef* harbored a primary determinant of pathogenicity in these Tg mice and that the other known HIV-1 genes were dispensable for the appearance of the phenotype.

### Tg RNA Expression in CD4C/HIV$^{Mut}$ Mice

Northern blot analysis showed that the three main transcripts of HIV-1 (8.8 kb full-length, 4.3 kb env-specific, and the 2.0 kb multiply-spliced) were detected at higher levels in lymphoid than in nonlymphoid organs, in all Tg mutant mice (Figure 2A). The Tg expression was correctly regulated in all founders, being consistent with the tissue specificity of this CD4C promoter (Hanna et al., 1994, 1998). Weaker Tg expression was detected in kidney, lungs, intestine, and liver, most likely reflecting expression in T lymphocytes and/or resident macrophages, as previously documented (Hanna et al., 1998) and as reconfirmed in the present study (see below). Expression was not detected in testis, skin, and muscle (data not shown). This pattern of expression was indistinguishable from that observed previously in CD4C/HIV$^{wt}$ mice (Hanna et al., 1998). As expected, the levels of Tg RNA expression varied from founder line to another, most likely reflecting a positional effect at the site of Tg insertion (Figures 2B and 2C). An excellent correlation between the levels of Tg RNA expression and the time of death ($TD_{50}$) was observed in mice from the CD4C/HIV$^{MutA}$, CD4C/HIV$^{MutB}$, and CD4C/HIV$^{MutG}$ lines (Figure 3E).

### Tg HIV-1 Protein Expression in CD4C/HIV$^{Mut}$ Mice

Western blot analysis of lymphoid organs from different mutant mice was performed with anti-nef and anti-env antibodies. This analysis revealed the presence of the Nef protein in lymphoid tissues of mice harboring an

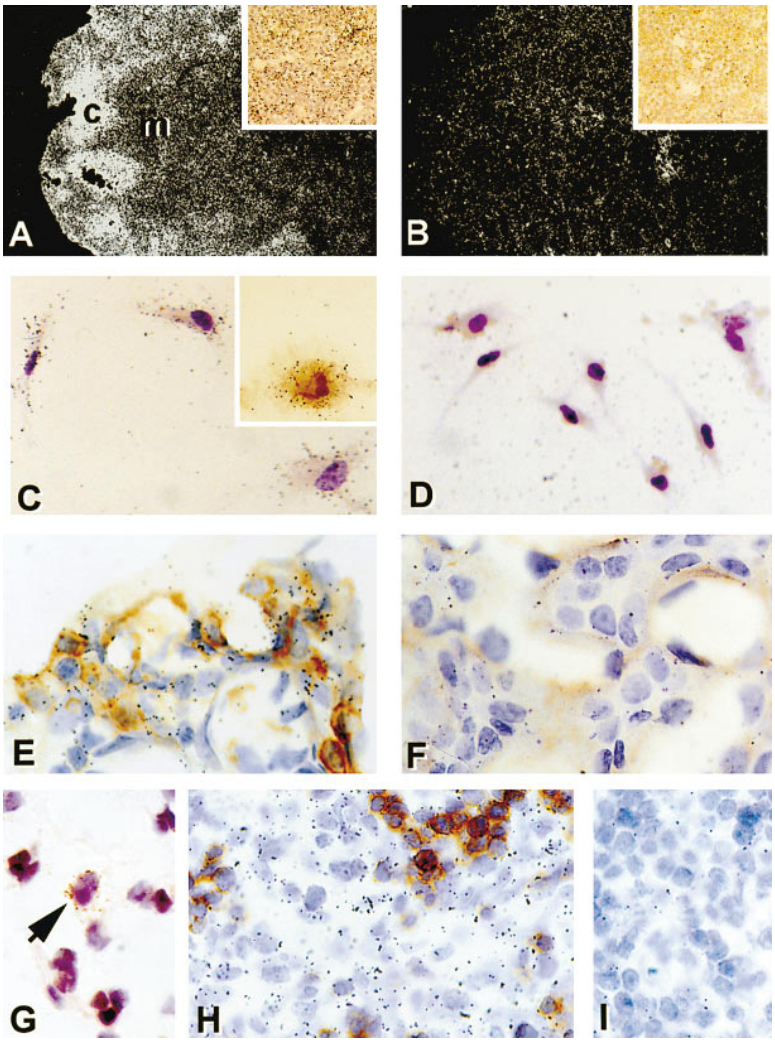


Figure 4. Detection of Tg Expression in CD4C/HIV$^{Mut}$ Tg Mice by ISH

Tg expression was detected by ISH with HIV-1-specific riboprobes. (A) Thymus in darkfield of a CD4C/HIV$^{MutG}$ (F27367) animal hybridized with HIV-1 antisense probe. Expression is higher in cortex (c) than in medulla (m) (and inset [brightfield]).

(B) An adjacent section to that shown in (A), hybridized with HIV-1 sense probe as control. Insets to (A) and (B); histology of medulla. Note ISH reaction associated with cells of lymphoid morphology (A).

(C–F) Tg expression was detected in macrophages from CD4C/HIV$^{MutG}$ mice. Plated peritoneal macrophages either processed for ISH alone (C) or double labeled with $\alpha$-Mac-1/ISH (inset to C) were positive for Tg expression. (D) Peritoneal macrophages hybridized with sense probe and exposed to only secondary antibody. (E) A small mononoclear cell infiltrate in kidney was double labeled with $\alpha$-Mac-1/ISH. The majority of Mac-1 positive cells are positive for HIV-1 RNA. (F) Negative control for (E) (same treatment as [D]).

(G) High power of lung alveoli from a CD4C/HIV$^{MutB}$ mouse (F26622) processed for ISH and showing Tg expression in an alveolar macrophage (arrow).

(H) The spleen from a CD4C/HIV$^{MutG}$ mouse (F27367) was double labeled with $\alpha$-B220/ISH. B220$^{+}$ B cells do not express high levels of HIV-1 RNA.

(I) Negative control for (H) (same treatment as [D]). Counterstain: hematoxylin and eosin (H&E) (A, B, and G) or hematoxylin alone (C–F, H, and I).

Magnifications: (A and B): 43×; (C, D, and G): 250×; (E and F): 360×; (H and I): 340×; insets to (A and B): 150×; and to (C): 400×.

intact HIV-1 *nef* gene (CD4/HIV$^{MutA}$, CD4C/HIV$^{MutB}$, and CD4C/HIV$^{MutG}$) (Figure 3A), as expected. Similarly, the expected gp160 and gp120 HIV-1 env proteins were detected in lymphoid organs of CD4/HIV$^{MutA}$, CD4C/HIV$^{MutC}$, and CD4C/HIV$^{MutH}$ Tg mice (Figure 3C). These HIV-1 proteins could not be detected in target organs of mice harboring a mutated gene. In Tg mouse lines expressing lower levels of Tg RNA, HIV-1 env and Nef proteins could not be detected by this method.

HIV-1 gag CA(p24) protein was detected by ELISA on thymuses and spleens of mice from both CD4C/HIV$^{MutB}$ and CD4C/HIV$^{MutH}$ founder lines, with higher levels observed in lines expressing higher levels of Tg RNA (Figure 3D). These results indicated that the expected HIV-1 proteins were produced in these Tg mice.

### Tg Expression Correlates with the Latency of Disease

The higher Tg expression in lines exhibiting the most acute phenotype suggested that this was an important biological parameter. Further analysis showed a very strong correlation between the levels of RNA, Nef, and p24 proteins and the $TD_{50}$ values (Figure 3E). The data appear to fit a biphasic curve, indicating that below a certain protein level (arbitrarily defined here as 14-fold or $\sim$135 $\pm$ 50 pg p24/mg of total thymus protein), the rate at which disease developed was relatively slow. However, above this level, disease progression was much faster and followed a very steep curve, with a different kinetics. Furthermore, a second threshold of Tg expression was observed, below which no disease developed within 1 year. Therefore, our data suggest that disease progression in these Tg mice is highly dependent on the levels of intracellular Nef proteins.

### Tg Expression Evaluated by *In Situ* Hybridization (ISH)

The organ and cell type–specific patterns of Tg expression detected in the CD4C/HIV$^{Mut}$ Tg mice by ISH with $^{35}$S-labeled HIV-1-specific riboprobes (Figure 4) were very similar to those previously described for the CD4C/HIV$^{wt}$ Tg mice (Hanna et al., 1998). Briefly, thymic expression of the Tg was most concentrated in the cortical region and to a lesser extent in medullary cells (Figure 4A), consistent with expression in immature CD4$^{+}$CD8$^{+}$ (cortical) and in mature CD4$^{+}$CD8$^{-}$ (medullary) T cells. In spleen, Tg expression was concentrated in the red pulp and marginal zone of the white pulp (data not shown). Tg expression was also observed in non-lymphoid tissues. In the kidney, interstitial infiltrating

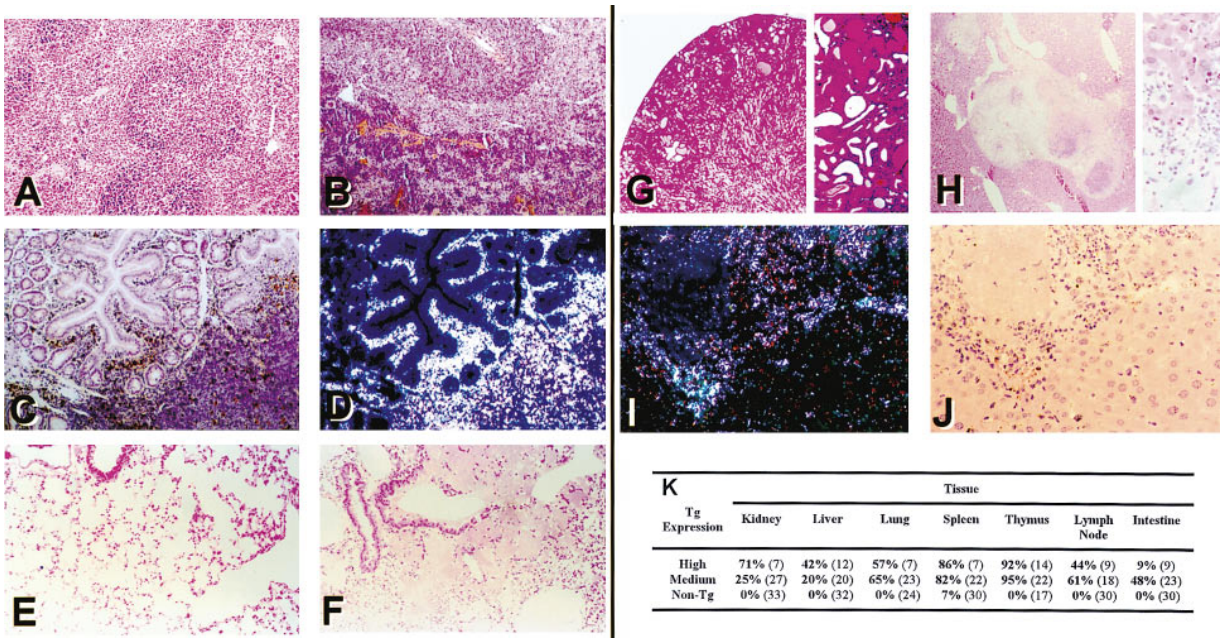


K

| Tg Expression | Tissue | | | | | | |
|---|---|---|---|---|---|---|---|
| | Kidney | Liver | Lung | Spleen | Thymus | Lymph Node | Intestine |
| High | 71% (7) | 42% (12) | 57% (7) | 86% (7) | 92% (14) | 44% (9) | 9% (9) |
| Medium | 25% (27) | 20% (20) | 65% (23) | 82% (22) | 95% (22) | 61% (18) | 48% (23) |
| Non-Tg | 0% (33) | 0% (32) | 0% (24) | 7% (30) | 0% (17) | 0% (30) | 0% (30) |

Figure 5. Pathology and HIV-1 Transgene Expression in CD4C/HIV$^{Mut}$ Tg Mice

(A and B) Spleens from control non-Tg (A) and CD4C/HIV$^{MutA}$ Tg (F21380) (B) mice. Note the extensive loss of architecture and accumulation of fibrous tissue in (B).

(C) Histology of small intestinal mucosa from a CD4C/HIV$^{MutA}$ Tg mouse (F21388) showing the epithelium and lymphoid follicle.

(D) Darkfield image of the same field. The section has been processed for ISH and HIV-1-expressing cells are seen in both the lamina propria and the lymphoid follicle.

(E) Lung from a normal non-Tg mouse.

(F) Lung from a 12−month-old CD4C/HIV$^{MutG}$ (F27367) Tg animal showing both an interstitial pneumonitis and an extensive intra-alveolar exudate.

(G) Kidney from a CD4C/HIV$^{MutG}$ animal (F26990) showing severe tubulo-interstitial disease with widespread tubular atrophy and accumulation of proteinacous material in dilated tubules (inset).

(H) Necrotizing granuloma in the liver of a CD4C/HIV$^{MutB}$ (F26622) mouse. Note the surrounding normal liver tissue. Inset to (H): Wall of the granuloma composed of mononuclear cells consistent with the morphology of lymphocytes, macrophages, and occasional polymorphonuclear leucocytes.

(I) Darkfield image of liver granuloma from a CD4C/HIV$^{MutB}$ (F26622) animal processed for ISH. HIV-1-expressing cells are seen in the inflammatory cells at the periphery of the granuloma.

(J) Histology of the same field as (I).

(K) Incidence of histopathology observed in CD4C/HIV$^{Mut}$ Tg mice. High- (F21407, F26605, F26990) or medium- (F21380, F21388, F26622, F27367, F27011) expresser Tg mice, as shown in Figure 3E. In parenthesis, the number of Tg mice analyzed. Some non-Tg spleens had pathological changes that resembled the mildest pathology observed in Tg mice. Thymic atrophy was scored macroscopically. In the majority of mice (32/36), no thymic tissue was available for histology.

Counterstain of all panels, H&E.

Magnifications: (A–D): 50×; (E and F): 140×; (G and H): 48×; (I and J): 230×; insets to (G): 180× and to (H): 230×.

mononuclear cells (Figure 4E) and cells of unknown identity within glomeruli (data not shown) expressed the Tg. Infiltrating mononuclear cells expressing the Tg were also found in the lamina propria of the intestine (Figure 5D), in the liver (Figure 5I), and in the lung (data not shown). Liver Kuppfer cells (data not shown), lung alveolar macrophages (Figure 4G), peritoneal macrophages (Figure 4C), and kidney infiltrating macrophages (Figure 4E) (the latter two identified with α-Mac-1 immunostaining) were positive for Tg expression. However, several other cell types were negative for Tg expression: B cells, as identified with α-B220 (Figure 4H), endothelial cells, smooth muscle and connective tissue cells, myocytes of the heart and of skeletal muscle, seminiferous tubules, spermatocytes, and various epithelial cells, including epithelial cells of the gastrointestinal tract, renal tubular epithelial cells, pneumocytes, and hepatocytes (data not shown). Together, these results are consistent with the specificity of the CD4C promoter, as assessed previously (Hanna et al., 1994, 1998) for CD4$^+$ T cells and for cells of the macrophage/dendritic lineage.

### Pathological Assessment of CD4C/HIV$^{Mut}$ Tg Mice

Macroscopic examination revealed severe wasting, edema, and atrophy of all lymphoid organs (thymus, spleen, and lymph nodes) in a high proportion of the CD4C/HIV$^{MutA}$, CD4C/HIV$^{MutB}$, and CD4C/HIV$^{MutG}$ diseased Tg mice. These pathological changes were similar to those observed previously in CD4C/HIV$^{wt}$ Tg mice (Hanna et al., 1998). Control non-Tg littermates and CD4C/HIV$^{MutC}$ and CD4C/HIV$^{MutH}$ mice did not exhibit these abnormalities.

Histological examination also revealed changes indistinguishable from those observed previously in CD4C/HIV$^{wt}$ Tg mice (Hanna et al., 1998) and present at high

Table 1. Quantitation of Cells of Lymphoid Organs of Control and CD4C/HIV$^{Mut}$Tg Mice

| Mouse Line[a] | Number of Cells ($\times 10^6$) | | |
|---|---|---|---|
| | Thymus | Spleen | Mes. Lymph Nodes |
| Non-Tg | 70.9 ± 23 | 61.9 ± 20.8 | 20.3 ± 10.6 |
| CD4C/HIV$^{MutA}$ | | | |
| F21407 | ND[b] | 5.2 ± 4.2* | 1.1 ± 1.3* |
| F21380/21388[c] | 32.7 ± 30* | 33.1 ± 26.5* | 9.2 ± 9.3* |
| CD4C/HIV$^{MutB}$ | | | |
| F26605 | ND[b] | 26.2 ± 25.2* | 3.5 ± 5* |
| F26622 | 20.4 ± 7.1* | 14.4 ± 13.11* | 3.5 ± 2.9* |
| F26132 | 77.6 ± 33.4 | 60.1 ± 14.5 | 7.4 ± 2.4* |
| CD4C/HIV$^{MutC}$ | | | |
| F22564/(22568)[c] | 56.3 ± 13.6 | 56.7 ± 7.4 | 13 ± 10.1 |
| CD4C/HIV$^{MutG}$ | | | |
| F26990 | 7.2* | 8.1* | 5.4* |
| F27367 | 24.4 ± 1.6* | 30.8 ± 15* | 5.1 ± 2.4* |
| F27372/27011[c] | 61.7 ± 26.5 | 67.8 ± 24 | 16.4 ± 12.4 |
| CD4C/HIV$^{MutH}$ | | | |
| F37434 | 63.8 ± 22.5 | 74.2 ± 24.5 | 32.75 ± 12.7 |

* $p < 0.05$ by using Student's t test. ND, not determined.
[a] At least five mice of each line, except for line F62990 (one mouse), were analyzed.
[b] The thymus of these mice was so atrophied that no cells were recovered.
[c] Results of two founder lines, which express similar protein levels, except CD4C/HIV$^{MutC}$, were pooled.

frequency in medium- and high-expresser Tg mice (Figure 5K). Briefly, these diseased mice exhibited (1) severe depletion of the thymocytes and peripheral lymphocytes accompanied by loss of architecture of the lymphoid organs and fibrosis (Figure 5B); in some lymph nodes, there was a virtually complete burn out of the T cell zone, leaving only cortical follicles (B cells) (data not shown); (2) interstitial pneumonitis (Figure 5F); and (3) tubulo-interstitial nephritis, with marked tubular atrophy and dilatation and interstitial mononuclear infiltration (Figure 5G). This kidney pathology was more often seen in lines in which the Tg was highly expressed (Figure 5K).

In addition, novel pathologies were observed in some CD4C/HIV$^{MutA}$, CD4C/HIV$^{MutB}$, and CD4C/HIV$^{MutG}$ mice in which Tg expression was moderate and which survived longer (>4 months). These lesions potentially resulted from a more chronic course of disease. Thus, the lung pathology in some animals progressed to include an often extensive intra-alveolar exudate (Figure 5F). Livers were found with necrotizing granulomas (Figure 5H). The extent of these granulomas varied from a few small focal lesions in some animals to numerous and sometimes extensive lesions in other animals. Finally, hyperplasia of the lymphoid follicles of the intestinal mucosa was seen (Figure 5C). These were occasionaly associated with an infiltration of the lamina propria with mononuclear cells. Again, such pathological changes were not observed in control non-Tg littermates nor in CD4C/HIV$^{MutC}$ or CD4C/HIV$^{MutH}$ Tg mice.

### Analysis of Lymphoid Cells from CD4C/HIV$^{Mut}$ Tg Mice

Quantitation of cell numbers in the lymphoid organs of diseased mice showed a severe depletion relative to age-matched controls, especially in Tg mice exhibiting high levels of Tg expression (Table 1). In mice expressing moderate levels of CD4C/HIV$^{MutA}$, CD4C/HIV$^{MutB}$, and CD4C/HIV$^{MutG}$ Tg, and which became diseased later, the total cell number was normal at an early stage (data not shown) and became progessively depleted later.

FACS analysis was performed on thymocytes and on cells of the peripheral lymphoid system (blood, spleen, and mesenteric lymph nodes [LN]) with antibodies against various cell surface markers for T cells (CD4, CD8, TcR$\alpha\beta$, and Thy 1.2) and B cells (B220). For CD4/HIV$^{MutC}$ or CD4/HIV$^{MutH}$ Tg mice that remained in apparent good health, the results of FACS analysis were indistinguishable from those of the non-Tg littermates (Tables 2 and 3). However, mice from CD4/HIV$^{MutA}$, CD4/HIV$^{MutB}$, and CD4/HIV$^{MutG}$ lines all exibited similar abnormal profiles.

In the thymus, a decrease of the CD4 staining (Mean Fluorescence) of the single- ($CD4^+CD8^-$) and double- ($CD4^+CD8^+$) positive cells could be observed at an early stage, even before a loss of cells could be documented (Table 2 and Figure 6A). The percentage of $CD4^+CD8^+$ and $Thy1.2^+$ populations were not significantly different from those of non-Tg littermates, even in thymuses with significant cell loss. However, in the medium- and high-expresser Tg mice, a decrease of the $CD4^+CD8^-$ and of the $TcR^{high}$ positive T cells, which represent the mature T cells, could be observed (Table 2, Figure 6A).

The same analysis performed on peripheral lymphoid cells (spleen, blood [data not shown], mesenteric LN [Table 3 and Figure 6B]) also showed a progressive decrease of the CD4 (but not of the Thy1.2) cell surface mean fluorescence, which was sometimes reflected by the appearance of $CD4^{Low}$ and $CD4^{High}$ cells (see Figure 6B, F27011; mean fluorescence, Table 3). In addition, at an early stage, in medium- or high-expresser mice, a depletion of $Thy1.2^+$ T cells and, more specifically, of the $CD4^+$ T cells often accompanied by an increase of $CD8^+$ T cells, could be observed. This increase of the $CD8^+$ T cells was best seen in mesenteric LN of medium-expresser mice and was less often observed in the spleen. The CD4/CD8 ratio was significantly decreased in these mice (Table 3). At a later stage, particularly in

Table 2. Thymic Cell Surface Marker Analysis in CD4C/HIV$^{Mut}$ Tg Mice

| Mouse Line[a] | Cell populations (%) | | | | Mean Fluorescence (%) | |
|---|---|---|---|---|---|---|
| | Thy 1.2 | $CD4^+CD8^+$ | $CD4^+CD8^-$ | $CD4^-CD8^+$ | Thy 1.2 | CD4 |
| Non-Tg | 91.4 ± 8.4 | 83.2 ± 7.4 | 9.6 ± 3.3 | 4.7 ± 1.7 | 100 | 100 |
| CD4C/HIV$^{MutA}$ | | | | | | |
| F21380/21388 | 91.1 ± 7.2 | 79.6 ± 8.6 | 5.5 ± 1.3* | 6 ± 3.9 | 101.6 ± 9.2 | 39.8 ± 24* |
| CD4C/HIV$^{MutB}$ | | | | | | |
| F26622 | 95.3 ± 2.3 | 83.8 ± 7.3 | 3.7 ± 1.1* | 6.85 ± 2.2* | 104.9 ± 31.5 | 31.5 ± 12* |
| F26132 | 93.6 ± 5.1 | 84.2 ± 5.7 | 11.3 ± 3 | 5.5 ± 2.4 | 108.9 ± 19 | 104.6 ± 8.8 |
| CD4C/HIV$^{MutC}$ | | | | | | |
| F22564/22568 | 92.2 ± 4.8 | 81.6 ± 10.4 | 9.3 ± 3.2 | 4.7 ± 1.2 | 99.5 ± 21.4 | 97.9 ± 13 |
| CD4C/HIV$^{MutG}$ | | | | | | |
| F27367 | 93.5 ± 2.1 | 82.3 ± 1.9 | 8.9 ± 0.3 | 9.1 ± 1.1* | 94.6 ± 3.5 | 22.3 ± 0.6* |
| F27372/27011 | 96.2 ± 1.4 | 87.6 ± 4.7 | 4.8 ± 2.2* | 5.4 ± 1.4 | 90.9 ± 11.7 | 35.7 ± 1.8* |
| CD4C/HIV$^{MutH}$ | | | | | | |
| F37434 | 95.8 ± 1.3 | 82.7 ± 9.3 | 11.2 ± 2.1 | 4.7 ± 1.2 | 91.7 ± 6.4 | 94.8 ± 11.4 |
| F37435 | 97.1 ± 0.5 | 81.9 ± 0.4 | 11.7 ± 0.6 | 5.76 ± 0.8 | 107.2 ± 5.7 | 97.3 ± 0.6 |

* $p < 0.05$ by using Student's t test.
[a] At least five mice per line, except for line F37435 (four mice), were analyzed.

medium- or high-expresser mice, the numbers of both $CD4^+$ and $CD8^+$ T cells were dramatically reduced. The proportion of B220+ B cells in the peripheral organs was found to be increased in these three mutant mice relative to their control non-Tg littermates, possibly reflecting the T cell depletion in these organs.

The lymphoproliferative capacity of the lymphoid cells of CD4C/HIV$^{MutG}$ (F27367) Tg mice was also assessed before they showed signs of clinical disease. Anti-CD3 stimulated total spleen and mesenteric LN cells from these mice showed a decrease $^3$H-thymidine incorporation at only 25.6 ± 15.4% (n = 4) and 35.8 ± 25.1% (n = 4), respectively (corrected for T cell loss), of the control non-Tg littermates, indicating functional defects of T cells in these mice. The same spleen and LN cells stimulated with LPS proliferated at 110 ± 33% (n = 4) and 170 ± 132% (n = 4) of the control, respectively.

### Hematological Parameters of CD4C/HIV$^{Mut}$ Tg Mice

The hemoglobin, hematocrit, number of red and white blood cells, and platelets, as well as the percentage of monocytes, eosinophils, and basophils was not significantly different in non-Tg and Tg mice from all lines (data not shown). However, the percentage of lymphocytes was lower, as expected, in diseased Tg mice from CD4C/HIV$^{MutA}$, CD4C/HIV$^{MutB}$, and CD4C/HIV$^{MutG}$ high- and medium-expresser lines (25.3 ± 10.6%, n = 15) than in low-expresser or control non-Tg mice (56.3 ± 12.0%, n = 17). Also, the percentage of neutrophils was increased in moderate- and high-expresser Tg mice from the same lines (61.6 ± 10%, n = 15) as compared to low-expresser or non-Tg mice (37.3 ± 10.2%, n = 17).

As reported before for the CD4C/HIV$^{wt}$ Tg mice, the total serum immunoglobulin (Ig) levels (mg/ml) were also much lower (3.86 ± 4, n = 11) in diseased CD4C/HIV$^{MutA}$, CD4C/HIV$^{MutB}$, and CD4C/HIV$^{MutG}$ high-expresser Tg mice than in non-Tg mice (29 ± 8, n = 15). In mice expressing the same Tg at medium or low levels, the levels of total Ig were more variable, being either reduced (7.4 ± 4.8) in 25% (9/36) of Tg mice, elevated (70 ± 14) in 17% (6/36) of Tg mice, or unchanged (28.1 ± 10) in 58% (21/36) of Tg mice as compared to non-Tg controls. This

Table 3. Mesenteric Lymph Node Cell Surface Marker Analysis in CD4C/HIV$^{Mut}$ Tg Mice

| Mouse line (a) | Cell populations (%) | | | | CD4/CD8 Ratio | Mean Fluorescence (%) | |
|---|---|---|---|---|---|---|---|
| | Thy 1.2 | $CD4^+$ | $CD8^+$ | B220 | | Thy 1.2 | CD4 |
| Non-Tg | 63.1 ± 12.4 | 52.5 ± 7.8 | 18.8 ± 4.8 | 21.4 ± 7.1 | 2.94 ± 0.7 | 100 | 100 |
| CD4C/HIV$^{MutA}$ | | | | | | | |
| F21407 | 31.1 ± 0* | 24 ± 15.2* | 18.7 ± 8.4 | 31.1 ± 18.2* | 1.46 ± 0.8* | 112.7 ± 14.8 | 45.2 ± 23* |
| F21386/21388 | 42.3 ± 7.8* | 18.5 ± 6.9* | 24.6 ± 7.2* | 40.2 ± 9.2* | 0.81 ± 0.38* | 111.2 ± 8.4 | 24.4 ± 8.8* |
| CD4C/HIV$^{MutB}$ | | | | | | | |
| F26605 | 9.1 ± 6.6* | 3.47 ± 3.8* | 5.12 ± 2.6* | 60.8 ± 22* | 0.71 ± 0.8* | 101.9 ± 9.5 | 48 ± 16.7* |
| F26622 | 44.8 ± 6.6* | 17.74 ± 3* | 31.5 ± 13.9* | 28.9 ± 9.2 | 0.63 ± 0.3* | 89.3 ± 9.2 | 22.1 ± 8.4* |
| F26132 | 57.2 ± 10.4 | 42.4 ± 6.2* | 23 ± 7.9 | 30.4 ± 11.3* | 2.13 ± 1 | 108.1 ± 5.9 | 43.8 ± 5.9* |
| CD4C/HIV$^{MutC}$ | | | | | | | |
| F22564/22568 | 66.6 ± 6.7 | 53.7 ± 10.6 | 19.67 ± 4.2 | 17.6 ± 4.8 | 2.9 ± 1 | 111 ± 22.1 | 99.5 ± 20.2 |
| CD4C/HIV$^{MutG}$ | | | | | | | |
| F26990 | 24* | 14.63* | 8.4* | 68* | 1.74* | 89.5 | 76.8* |
| F27367 | 53.5 ± 8* | 20.1 ± 6.7* | 30.6 ± 4.1* | 34.1 ± 7.8* | 0.69 ± 0.32* | 89.4 ± 1.20 | 13.6 ± 8.7* |
| F27372/27011 | 50 ± 4.8* | 29.5 ± 4.5* | 27.1 ± 5.8* | 37.3 ± 5.3* | 1.15 ± 0.37* | 113.2 ± 18.7 | 35.2 ± 11.9* |
| CD4C/HIV$^{MutH}$ | | | | | | | |
| F37434 | 63.4 ± 3.2 | 53.4 ± 6 | 16.9 ± 2 | 25.4 ± 6.5 | 3.2 ± 0.6 | 96.9 ± 11.8 | 96.4 ± 15.5 |
| F37435 | 69 ± 6.5 | 50.8 ± 6.1 | 25.1 ± 2.3 | 21.1 ± 7.8 | 2.03 ± 0.03 | 108.9 ± 16.6 | 104.1 ± 25.2 |

* $p < 0.05$ by using Student's t test.
[a] At least five mice per line, except for lines F37435 (four mice) and F26990 (one mouse), were analyzed.

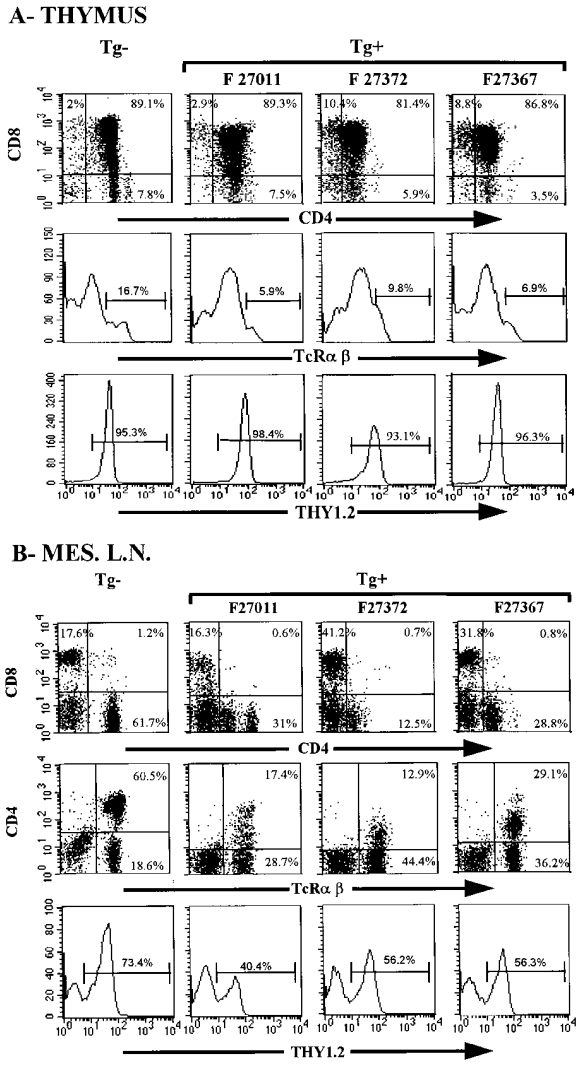


Figure 6. Flow Cytofluorometric Analysis of T Cell Subsets from CD4C/HIV$^{MutG}$ Tg Mice

Thymus (A) and mesenteric LN (B) cells from a non-Tg mouse and from three representative mice each from a different founder CD4C/HIV$^{MutG}$ Tg line were analyzed by flow cytometry for the expression of CD4, CD8, Thy1.2, and TcR$\alpha\beta$. The percentage of cells found in each quadrant are indicated. $10^4$ cells were analyzed.

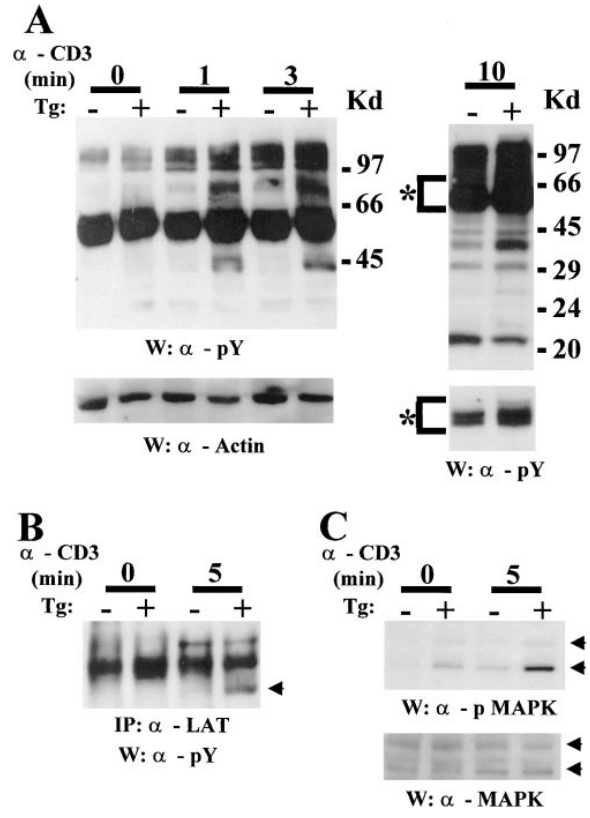


Figure 7. Detection of Tyrosine Phosphorylated Proteins in Thymocytes of CD4C/HIV$^{MutG}$ Tg Mice

Lysates from thymocytes of non-Tg or CD4C/HIV$^{MutG}$ Tg mice were prepared after stimulation with $\alpha$-CD3 for the indicated times.
(A) Lysates ($5 \times 10^5$ cells) were probed by protein immunoblotting first with anti-phosphotyrosine antibodies (4G10) ($\alpha$-pY). The asterisk indicates two exposures times of the film. The membrane was then washed and reprobed with anti-actin as a control for protein loading.
(B) Lysates from thymocytes ($5 \times 10^6$ cells) were immunoprecipitated with antibodies for LAT. Immune complexes were resolved on SDS-PAGE and blotted with $\alpha$-pY antibodies. The arrow shows LAT.
(C) Lysates ($5 \times 10^5$ cells) were probed first with anti-phospho p44/p42 MAP Kinase antibodies and then washed and reprobed with anti-MAP Kinase antibodies. The arrows show p42 and p44 MAPK.

variation did not seem to correlate with the clinical disease phenotype. As expected, mice from CD4C/HIV$^{MutC}$ and CD4C/HIV$^{MutH}$ founders had Ig levels ($31 \pm 10$, $n = 13$) not significantly different from those of control non-Tg mice ($29 \pm 8$, $n = 15$).

### Increased Constitutive and $\alpha$-CD3 Stimulated Tyrosine Phosphorylation in Thymocytes of CD4C/HIV$^{MutG}$ Tg Mice

To explore the mechanism of thymic perturbation and T cell loss in these Tg mice, we investigated the state of tyrosine phosphorylation after engagement of the T cell receptor (TcR) with $\alpha$-CD3. Thymocytes from CD4C/HIV$^{MutG}$ Tg mice showed a constitutive increase of tyrosine phosphorylation of several substrates as compared to thymocytes from non-Tg mice (Figure 7A). In addition, upon $\alpha$-CD3 stimulation, levels of tyrosine phosphorylation of several substrates were higher in Tg than in control non-Tg mice (Figure 7A). The pattern of the tyrosine phosphorylated proteins was virtually identical in Tg and non-Tg thymocytes, except for the quantitative differences. Identical results were obtained with thymocytes from CD4C/HIV$^{MutA}$ Tg mice (data not shown). Some proteins most hyperphosphorylated in Tg mice had an apparent mobility of 135, 120, 100, 70, 60, 45, and 36/38 kDa and the latter species was especially evident. Several of the proteins whose tyrosine phosphorylation is enhanced following TcR engagement have been identified (Weiss and Littman, 1994). One of them, LAT (36/38 kDa), is of special interest since it links the TcR to cellular activation (Zhang et al., 1998). Our analysis showed that LAT was hyperphosphorylated in CD4C/HIV$^{MutG}$ Tg mice after $\alpha$-CD3 stimulation (Figure 7B). In addition, the phosphorylation state of p44/p42 MAP Kinase (Erk-1/Erk-2) was also found to be increased in

thymocytes of CD4/HIV$^{MutG}$ (Figure 7C) and CD4C/HIV$^{MutA}$ (data not shown) Tg mice, as compared to non-Tg littermates. This enhanced tyrosine phosphorylation state was observed both constitutively and after α-CD3 stimulation. Together, these results show that thymocytes from CD4C/HIV$^{MutG}$ Tg mice are in a state of activation and of α-CD3 hyperresponsiveness.

## Discussion

### HIV-1 Nef Harbors a Major Determinant of Pathogenicity in Tg Mice

Our mutational analysis revealed that an AIDS-like phenotype could be induced in Tg mice by the expression of a single HIV-1 gene, *nef*, in CD4$^+$ T cells and in cells of the monocyte/macrophage lineage. The other known HIV-1 genes were dispensable for the emergence of this phenotype. This result was rather surprising in view of the fact that profound effects on host cell functions have previously been reported to be induced in vitro by other HIV-1 proteins, more specifically by Vpr (Rogel et al., 1995; Levy et al., 1993), Vpu (Willey et al., 1992), Tat (Viscidi et al., 1989; Li et al., 1995), and the envelope gp120 and gp41 glycoproteins (Siliciano, 1996). However, the *vpr*, *vpu*, *tat*, and *env* genes were dispensable for the development of the disease in CD4C/HIV$^{Mut}$ Tg mice. Since some of these genes have previously been reported to induce impressive phenotypes, not only in vitro but also in vivo in Tg mice (for review see Klotman et al., 1995), this suggests that the cell type in which some HIV-1 proteins are expressed is a major factor in determining their effect. The apparent inability of env gp120 to affect disease development may be related to the absence of its proper receptor (the human CD4 protein) or its coreceptors in these mice.

In other related studies, HIV-1 *nef* was expressed in T cells of Tg mice using the promoter/enhancer elements of the CD3δ (Skowronski et al., 1993), CD2 (Brady et al., 1993), or TcR β chain (Lindemann et al., 1994) gene. In some of these Tg mice, a severe immunodeficiency with loss of T cells and alterations of T cell activation was observed. However, none of these nef Tg mice developed a multi-organ syndrome and an immune disease similar to the one observed in CD4C/HIV$^{MutG}$ Tg mice and which most closely mimics human AIDS, as discussed previously (Hanna et al., 1998). The different phenotypes observed in the CD4C/HIV$^{MutG}$ Tg mice studied here are likely to reflect the cell type(s) expressing the Tg, namely the CD4$^+$ T cell subset and cells of the monocyte/macrophage lineage. These are the same cells as those found infected in HIV-1-positive individuals (Pantaleo and Fauci, 1995). The differences in the levels of Tg expression in CD4C/HIV$^{Mut}$ Tg mice and in the other *nef*-expressing Tg mice are unlikely to explain the different phenotypes observed, since the same AIDS-like disease developed, but after longer latent periods, in CD4C/HIV$^{Mut}$ Tg mice expressing the Tg at lower levels.

The mechanism by which these various phenotypes are induced in CD4C/HIV$^{Mut}$ Tg mice is likely to be complex. We have explored TcR signaling events in Tg thymus and found that Nef-expressing thymocytes were in a state of activation and hyperresponsiveness with respect to the tyrosine phosphorylation of several substrates of TcR signaling, including some involved in early (LAT) and late (MAP Kinase) events. Interestingly, LAT is a substrate for the ZAP-70 tyrosine kinase and binds to several signaling molecules and, as such, serves as a linker to couple the TcR to downstream signaling events (Zhang et al., 1998). Nef has been found to bind to MAP kinase and to inhibit its kinase activity (Greenway et al., 1996). The enhanced tyrosine phosphorylation of the MAP Kinase seen in the CD4C/HIV$^{Mut}$ Tg mice would rather suggest that its enzyme activity is increased. Other previous studies on the effects of HIV-1 Nef in T cells in vitro has led to contradictory results either blocking or stimulating TcR signaling (Harris, 1996). In vivo, later events in TcR signaling (calcium mobilization and proliferation) were found to be stimulated (Skowronski et al., 1993). An enhanced constitutive and stimulated tyrosine phosphorylation similar to the one seen in CD4/HIV$^{MutG}$ Tg mice has not been reported in cells expressing wild-type HIV-1 Nef. If such a state of constitutive activation were present in HIV-1-infected human T cells, it may facilitate HIV-1 replication. This activation state may also be involved in thymic atrophy and T cell loss in the CD4C/HIV$^{Mut}$ Tg mice, since it mimics TcR induction, which is known to induce cell death (Kroemer, 1995). Therefore, our study may provide a molecular mechanism for the T cell loss in these Tg mice and shows that this animal model can be instrumental in studying the effects of Nef on TcR signaling in relevant primary target cells and in unraveling unique molecular defects induced by HIV-1.

### Does the Critical Role of *nef* in CD4/HIV Tg Mice Reflect its Role in the Human Disease?

The role of *nef* in HIV-1 infection has emerged from in vitro and clinical studies as well as from studies with the related primate lentivirus, the simian immunodeficiency virus (SIV). Nef has been shown to affect T cell signal transduction (Iafrate et al., 1997) and to downregulate human CD4 (Garcia and Miller, 1991) and MHC class I (Collins et al., 1998) proteins at the cell surface. This effect of Nef is not species-specific, and downregulation of mouse CD4 in primary cells of CD3δ/nef and CD2/nef Tg mice has been documented (Brady et al., 1993; Skowronski et al., 1993) and was confirmed here in the CD4C/HIV$^{MutG}$ Tg mice. Although dramatic, the biological significance of CD4 downregulation is not clear, nor is its role, if any, in the pathogenesis of this AIDS-like disease. Studies of Nef mutants unable to down-regulate CD4 (Iafrate et al., 1997) but competent in other functions should help in elucidating the role of this phenomenon in Nef-induced pathogenesis. Additionally, it is now well accepted that *nef* plays a positive role in enhancing virus replication in vitro, particularly in primary peripheral blood mononuclear cells and macrophages (Miller et al., 1994), and most importantly in vivo. In juvenile rhesus macaques and in the few patients infected, respectively, with *nef*-deleted SIV or HIV-1 mutant strains, viral loads remained low (Kestler et al., 1991; Deacon et al., 1995; Kirchhoff et al., 1995). In addition, and most importantly, both humans and primates infected with *nef*-deleted viruses failed to develop disease

after a long period of observation, strongly suggesting that *nef* is required for the pathogenecity of the virus (Kestler et al., 1991; Deacon et al., 1995; Kirchhoff et al., 1995). However, a role of *nef* independent of its role in the virus replication could not be unmasked in these experimental or clinical settings. Our results in Tg mice, where virus replication is absent, clearly show that indeed *nef* can play an independent role in target cells, apparently affecting them in such a way that a severe AIDS-like disease is induced.

The disease arising in the CD4C/HIV$^{MutG}$ Tg mice affects many organs. The induction of such numerous pathological changes in several organs of Tg mice following the expression of a single known gene product (Nef) suggests a common underlying mechanism for the multi-organ lesions. Since the Tg expression is largely restricted to CD4$^+$ T cells and cells of the monocyte/macrophage lineage, factor(s) released from one or some of these cell populations are likely to be involved in disease appearance in CD4C/HIV$^{MutG}$ Tg mice. In various Tg mouse target organs, the pathological lesions are strikingly similar to those found in human AIDS, especially pediatric AIDS (Calvelli and Rubinstein, 1990), as we previously discussed (Hanna et al., 1998). This is the case for early death (Enger et al., 1996), wasting (Coodley et al., 1994) and failure to thrive (Calvelli and Rubinstein, 1990), thymic atrophy, lymphadenopathy and preferential loss of CD4$^+$ T cells (Pantaleo and Fauci, 1995), tubulo-interstitial nephritis (Seney et al., 1990) and lymphoid interstitial pneumonitis (McSherry, 1996), which constituted the major lesions of the CD4C/HIV$^{Mut}$ Tg mice. Therefore, the remarkable similarities of these multi-organ lesions in CD4C/HIV$^{Mut}$ Tg mice and in human AIDS strongly suggest that Nef has similar, if not identical, effects in murine target cells, to its effects in human target cells. This possibility is reenforced by the fact that the effectors, which are known to interact with Nef (Harris, 1996), appear to be well conserved in mouse and man. If correct, this suggestion would imply that, as in CD4C/HIV$^{MutG}$ Tg mice, *nef* harbors an important determinant of pathogenicity of HIV-1 in humans and may be responsible for the major pathological manifestations of human AIDS. The mouse model developed here would be quite appropriate to assay the pathogenic potential of different *nef* alleles arising in infected individuals exhibiting distinct clinical courses. This novel function of *nef*, that is, its ability to induce an AIDS-like disease in Tg mice, may be most relevant to assay. The constitutive HIV-1 expression through the hCD4 regulatory sequences, although distinct from the LTR-driven viral expression, is likely to mimic a state of productive infection in human cells.

Furthermore, the profound influence of the levels of Nef expression on the latency of the AIDS-like disease of CD4/HIV$^{Mut}$ Tg mice suggests that this same parameter may also be critical in human AIDS. We previously noticed such a correlation while studying the CD4C/HIV$^{wt}$ Tg and chimeric mice (Hanna et al., 1998). The correlation is better documented here with the CD4C/HIV$^{Mut}$ Tg mice. The outcome of disease seems to depend entirely on the levels of the *nef* gene expression in the target cells. Even more interesting, our data indicate that disease progression follows two very distinct kinetics depending on whether the intracellular levels of Nef are above (fast progression) or below (slow progression) a certain threshold. If a similar phenomenon governs the progression of human AIDS, the strong correlation between the plasma viral load and progression to AIDS observed in humans (Ho, 1996) is likely to reflect the intracellular Nef concentrations in specific target cells. This possibly opens novel avenues for therapy.

## Experimental Procedures

### Transgene Construction and Generation of Tg Mice

The CD4C/HIV$^{Mut}$ transgenes were constructed by mutating the NL4–3 HIV-1 genome of the CD4C/HIV$^{wt}$ Tg (Hanna et al., 1998). The CD4C/HIV$^{MutA}$ Tg was generated by the addition of a 14-mer oligonucleotide containing three stop codons in each open reading frame (ORF) (5′-CTAGTCTAGACTAG-3′, "stop oligo") at the SphI (nucleotide [nt] 1447) and NdeI (nt 5123) sites of HIV-1$^{NL4-3}$ to produce *gag* and *vif* mutant genes, respectively. This oligo contains a XbaI site allowing the screening of mutated clones. The *pol* gene was mutated by deleting the 22 base pair (bp) HincII fragment (nt 2498–2521) followed by addition of the "stop oligo" at this site. DNAs with *vpr* or *vpu* gene mutation (deletion of nt 5622–5737 and nt 6062–6180, respectively) were available through the NIH AIDS Reagent Program as plasmids p210–19 and p210–13 (Gibbs et al., 1994). The *tat* mutation was produced by PCR site-directed mutagenesis using primer 297 (5′-CCAGGGCTATAGTCTAG-3′), containing G to T mutation at nt 5854, creating a stop codon. The CD4C/HIV$^{MutB}$ transgene was generated by the addition of "stop oligo" in the *env* gene at the NdeI site (nt 6400). The CD4C/HIV$^{MutC}$ transgene was constructed from mutA by interrupting the *nef* ORF. This was accomplished by filling the XhoI site (nt 8887) with Klenow. The CD4C/HIV$^{MutG}$ transgene was constructed from mutant A by interrupting the *rev* and *env* genes by introducing the "stop oligo" at the SacI (nt 6003) and NdeI (nt 6400) sites, respectively. The CD4C/HIV$^{MutH}$ transgene was generated by ligating the 6.5 kbp BssHII-NheI HIV-1 fragment from the CD4C/HIV$^{wt}$ DNA with the 3′-end 3.2kbp NheI-AatII fragment of the mutant C DNA containing the *nef* mutation. All mutations were screened by XbaI digestion whenever possible and confirmed by sequencing. All transgene DNAs were isolated from the vector by AatII digestion and purified to produce Tg mice, as described before (Hanna et al., 1998).

### Northern Analysis

Total RNAs were prepared from different tissues, and 10 μg was electrophoresed on formaldehyde agarose gels and processed for hybridization with the $^{32}$P-labeled 3.5 kbp SacI (3′ end) or 1.4 kbp HindIII-SacI (nef-specific) NL4–3 HIV-1 probe, as previously described (Hanna et al., 1998).

### Detection of HIV-1 Proteins

Detection of HIV-1 proteins by Western immunoblotting was performed as previously described (Goudreau et al., 1996). Polyclonal goat antibodies to gp160 (ERC-188) (1:5000) were obtained through the NIH AIDS Reagent Program. Polyclonal rabbit antibodies against Nef were obtained from V. Erfle (1:1000). Horse-radish peroxidase-conjugated secondary antibodies (goat or rabbit) were used at 1:6000 dilution. Proteins were detected using an enhanced chemiluminescent substrate (Amersham). The amount of protein in lysates was quantitated using a Micro BCA assay (Sigma). HIV-1 p24 gag proteins were quantified by using the Abbott HIVAG-1 Monoclonal ELISA kit, as previously described (Goudreau et al., 1996).

### Anti-Phosphotyrosine Immunoblotting

Thymocytes were stimulated with α-CD3 (145–2C11) (5 μg/ml) (Skowronski et al., 1993) and RIPA extracts made as previously described (Goudreau et al., 1996). Lysates were either untreated or immunoprecipitated with anti-LAT antibodies (Upstate Biotechnology [UBI]) and Protein G-Agarose (Boehringer) before electrophoresis on SDS-PAGE or directly run on gels and immunoblotted with α-phosphotyrosine (4G10) (UBI) or α-phospho p44/42 MAP kinase rabbit antibodies (New England Biolabs).

### Microscopic Analysis and ISH

Lymphoid and nonlymphoid organs were processed as previously described (Hanna et al., 1998) for microscopic assessment. ISH was performed on frozen or paraffin-embedded tissues or peritoneal macrophages as described previously (Goudreau et al., 1996).

### FACS Analysis and Proliferation Assays

FACS analysis and cell proliferation assays were performed on lymphoid cells prepared from Tg and non-Tg aged-matched littermates, as previously described (Huang et al., 1991; Hanna et al., 1998).

### Hematologic Parameters

Differential counts were performed on Wright's stained blood smears taken from Tg and non-Tg control animals. Analysis was also performed with the Instrument Technicon H.1 System (Bayer Co.). ELISAs for detection of total serum Ig levels were performed, as previously described (Hanna et al., 1998).

### Acknowledgments

This work was supported by grants to P. J. from the Medical Research Council of Canada. D. G. K. was the recipient of a career development award (chercheur-boursier) from the Fonds de la Recherche en Santé du Québec. We thank Nathalie Gauthier, Karina Lamarre, Benoît Laganière, Michel Robillard, Michel Ste-Marie, Martin Demers, and Ginette Massé for excellent technical assistance. We are grateful to Volker Erfle and Sylvain Meloche for providing anti-Nef and anti-MAPK antibodies and to Patrice Hugo, André Veillette, and Louise Larose for helpful discussions. We thank Scott Hughes for initial detection of HIV-1 proteins in some mice.

Received April 15, 1998; revised September 8, 1998.

### References

Brady, H.J., Pennington, D.J., Miles, C.G., and Dzierzak, E.A. (1993). CD4 cell surface downregulation in HIV-1 Nef transgenic mice is a consequence of intracellular sequestration. EMBO J. *12*, 4923–4932.

Calvelli, T.A., and Rubinstein, A. (1990). Pediatric HIV infection: a review. Immunodefic. Rev. *2*, 83–129.

Collins, K.L., Chen, B.K., Kalams, S.A., Walker, B.D., and Baltimore, D. (1998). HIV-1 Nef protein protects infected primary cells against killing by cytotoxic T lymphocytes. Nature *391*, 397–401.

Coodley, G.O., Loveless, M.O., and Merrill, T.M. (1994). The HIV wasting syndrome: a review. J. Acquir. Immune Defic. Syndr. *7*, 681–694.

Deacon, N.J., Tsykin, A., Solomon, A., Smith, K., Ludford-Menting, M., Hooker, D.J., McPhee, D.A., Greenway, A.L., Ellett, A., Chatfield, C., and et al. (1995). Genomic structure of an attenuated quasi species of HIV-1 from a blood transfusion donor and recipients. Science *270*, 988–991.

Enger, C., Graham, N., Peng, Y., Chmiel, J.S., Kingsley, L.A., Detels, R., and Munoz, A. (1996). Survival from early, intermediate, and late stages of HIV infection. JAMA *275*, 1329–1334.

Garcia, J.V., and Miller, A.D. (1991). Serine phosphorylation-independent downregulation of cell-surface CD4 by nef. Nature *350*, 508–511.

Gibbs, J.S., Regier, D.A., and Desrosiers, R.C. (1994). Construction and in vitro properties of HIV-1 mutants with deletions in "nonessential" genes. Aids Res. Hum. Retroviruses *10*, 343–350.

Goudreau, G., Carpenter, S., Beaulieu, N., and Jolicoeur, P. (1996). Vacuolar myelopathy in transgenic mice expressing human immunodefiency virus type 1 proteins under the regulation of the myelin basic protein gene promoter. Nat. Med. *2*, 655–661.

Greenway, A., Azad, A., Mills, J., and McPhee, D. (1996). Human immunodeficiency virus type 1 Nef binds directly to Lck and mitogen-activated protein kinase, inhibiting kinase activity. J. Virol. *70*, 6701–6708.

Hanna, Z., Simard, C., and Jolicoeur, P. (1994). Specific expression of the human CD4 gene in mature $CD4^+CD8^-$ and immature $CD4^+CD8^+$ T cells, and in macrophage of transgenic mice. Mol. Cell. Biol. *14*, 1084–1094.

Hanna, Z., Kay, D.G., Cool, M., Jothy, S., Rebai, N., and Jolicoeur, P. (1998). Transgenic mice expressing human immunodeficiency virus type 1 in immune cells develop a severe AIDS-like disease. J. Virol. *72*, 121–132.

Harris, M. (1996). From negative factor to a critical role in virus pathogenesis: the changing fortunes of Nef. J. Gen. Virol. *77*, 2379–2392.

Herskowitz, A. (1996). Cardiomyopathy and other symptomatic heart diseases associated with HIV infection. Curr. Opin. Cardiol. *11*, 325–331.

Ho, D.D. (1996). Viral counts count in HIV infection. Science *272*, 1124–1125.

Huang, M., Simard, C., Kay, D.G., and Jolicoeur, P. (1991). The majority of cells infected with the defective murine AIDS virus belong to the B cell lineage. J. Virol. *65*, 6562–6571.

Iafrate, A.J., Bronson, S., and Skowronski, J. (1997). Separable functions of Nef disrupt two aspects of T cell receptor machinery: CD4 expression and CD3 signaling. EMBO J. *16*, 673–684.

Kestler, H.W., Ringler, D.J., Mori, K., Panicali, D.L., Sehgal, P.K., Daniel, M.D., and Desrosiers, R.C. (1991). Importance of the nef gene for maintenance of high virus loads and for development of AIDS. Cell *65*, 651–662.

Kirchhoff, F., Greenough, T.C., Brettler, D.B., Sullivan, J.L., and Desrosiers, R.C. (1995). Brief report: absence of intact nef sequences in a long-term survivor with nonprogressive HIV-1 infection. N. Eng. J. Med. *332*, 228–232.

Klotman, P.E., Rappaport, J., Ray, P., Kopp, J.B., Franks, R., Bruggeman, L.A., and Notkins, A.L. (1995). Transgenic models of HIV-1. AIDS *9*, 313–324.

Kroemer, G. (1995). The pharmacology of T cell apoptosis. Adv. Immunol. *58*, 211–296.

Levy, D.N., Fernandes, L.S., Williams, W.V., and Weiner, D.B. (1993). Induction of cell differentiation by human immunodeficiency virus 1 vpr. Cell *72*, 541–550.

Li, C.J., Friedman, D.J., Wang, C., Metelev, V., and Pardee, A.B. (1995). Induction of apoptosis in uninfected lymphocytes by HIV-1 Tat protein. Science *268*, 429–431.

Lindemann, D., Wilhelm, R., Renard, P., Althage, A., Zinkernagel, R., and Mous, J. (1994). Severe immunodeficiency associated with a human immunodeficiency virus 1 NEF/3′-long terminal repeat transgene. J. Exp. Med. *179*, 797–807.

McSherry, G.D. (1996). Human immunodeficiency-virus-related pulmonary infections in children. Semin. Respir. Infect. *11*, 173–183.

Miller, M.D., Warmerdam, M.T., Gaston, I., Greene, W.C., and Feinberg, M.B. (1994). The human immunodeficiency virus-1 nef gene product: a positive factor for viral infection and replication in primary lymphocytes and macrophages. J. Exp. Med. *179*, 101–113.

Pantaleo, G., and Fauci, A.S. (1995). New concepts in the immunopathogenesis of HIV infection. Annu. Rev. Immunol. *13*, 487–512.

Price, R.W. (1996). Neurological complications of HIV infection. Lancet *348*, 445–452.

Rogel, M.E., Wu, L.I., and Emerman, M. (1995). The human immunodeficiency virus type 1 vpr gene prevents cell proliferation during chronic infection. J. Virol. *69*, 882–888.

Seney, F.D., Jr., Burns, D.K., and Silva, F.G. (1990). Acquired immunodeficiency syndrome and the kidney. Am. J. Kidney. Dis. *16*, 1–13.

Siliciano, R.F. (1996). The role of CD4 in HIV envelope-mediated pathogenesis. Curr. Top. in Microbiol. Immunol. *205*, 159–179.

Skowronski, J., Parks, D., and Mariani, R. (1993). Altered T cell activation and development in transgenic mice expressing the HIV-1 nef gene. EMBO J. *12*, 703–713.

Viscidi, R.P., Mayur, K., Lederman, H.M., and Frankel, A.D. (1989). Inhibition of antigen-induced lymphocyte proliferation by Tat protein from HIV-1. Science *246*, 1606–1608.

Weiss, A., and Littman, D.R. (1994). Signal transduction by lymphocyte antigen receptors. Cell *76*, 263–274.

Willey, R.L., Maldarelli, F., Martin, M.A., and Strebel, K. (1992). Human immunodeficiency virus type 1 Vpu protein induces rapid degradation of CD4. J. Virol. *66*, 7193–7200.

Zhang, W., Sloan-Lancaster, J., Kitchen, J., Trible, R.P., and Samelson, L.E. (1998). LAT: the ZAP-70 tyrosine kinase substrate that links T cell receptor to cellular activation. Cell *92*, 83–92.